

# IDeRS: Iterative Dehazing Method for Single Remote Sensing Image

## 1. APPENDIX-A: Atmospheric light Estimation

### 1.1. Recently atmospheric light estimation methods

Atmospheric light estimation has not been studied as extensively as priors for dehazing. For natural image dehazing (NID), with few exceptions, it is often estimated in an ad-hoc manner [1]. In early works the most haze-opaque pixel was used to estimate the atmospheric light. For example, Tan [7] chose the brightest pixel; and Fattal [8] used it as an initial guess for an optimization problem. However, the pixel with the highest intensity might correspond to a bright object rather than to the atmospheric light.

Recently, for natural image, there are five effective A estimating methods, which are illustrated in Table 1 in Appendix 1.3. To find the most accurate estimating method for remote sensing image dehazing (RSID), we testify these five algorithms both qualitatively and quantitatively.

### 1.2. Testings on atmospheric light estimating methods

Five well-known atmospheric light estimating algorithms, i.e. the DCP [2], Color-Line [3][4], Blind dehazing[5], DHNet [6] and Haze-Line [1] methods, are compared in our testing for RSID. In Fig.1, the hazy images are dehazed by our iterative dehazing method with different atmospheric light estimating algorithms. The estimated atmospheric light results are illustrated in the blocks on their corresponding dehazed images. The blocks on the hazy images are their manually extracted ground-truth atmospheric light. Quantitatively, we calculate the  $L_2$  error for each estimated atmospheric light result with the ground-truth. The mean  $L_2$ , median  $L_2$  and error variance are also calculated for deeper analyses. The quantitative results are illustrated in Fig.2.

For natural image, pixels at the deep depth or heavy haze region, which are known as the haze opaque pixels, is considered as the only light source of the image. Therefore, the haze opaque pixels can be used to estimate the atmospheric light in NID. However, the remote sensing image is obtained by the satellite sensors at downward-looking direction. The lowest-value region in transmission map no longer means the infinite distance from the sensors. Therefore, estimating atmospheric light using haze opaque pixel, such as the DCP [2] and DHNet [6] (in which the atmospheric light is preset as 1) is invalid for RSID. As Fig.2 demonstrates that, the DCP [2] and DHNet [6] have higher  $L_2$  errors than other methods. The misestimated atmospheric light may lead to color-distortion in the dehazed images, as illustrated in Fig.1(c) and (f).

The Color-Line [4] and the Blind [5] estimating methods can obtain relatively accurate atmospheric light without haze

opaque pixel. Their mean  $L_2$  errors are less than the DCP [2] and DHNet [6]. However, the error variance of these two methods, as well as the DCP [2] and DHNet [6], are larger than the Haze-Line method, meaning that their performance are not stable enough for RSID. That is, their performance depend on the extent the image adheres to the prior used by each method. Their dehazing results in Fig.1(c)-(f) also demonstrate this conclusion. Some of the results are acceptable (such as  $F_{a2}$  and  $F_{a3}$  of DCP [2] and Blind [5],  $F_{a3}$  and  $F_{a5}$  of Color-Line [4]), but for other images, their results are poor in dehazing performance, and some of them contribute severe color-distortions (such as  $F_{a2}$  and  $F_{a4}$  for Color-Line [4],  $F_{a4}$  for Blind [5] and DHNet [6]).

The method of Haze-Line estimating [1] is based on the haze-line prior [9]. That prior claims that pixels' intensities of objects with similar colors form lines in RGB space under haze. These lines intersect at the atmospheric light color, as illustrated in Fig.3. Using Hough transform, where the point with the highest vote is assumed to be the atmospheric light color. As running the Hough transform is computationally expensive, the authors proposed two techniques to accelerate the algorithm [1]. One is to work in 2D instead of 3D by projecting pixels' values on the RG, GB and RB planes. The second is to collect votes for a candidate atmospheric light only from cluster centers, rather than collecting votes from all pixels [1].

All of the errors and variances of Haze-Line [1][9] are significantly lower than other methods. That is, the Haze-Line atmospheric light estimating [1] outperforms other four methods' for non-sky remote sensing image. It can obtain the most accurate atmospheric light estimating.

Combining our iterative dehazing method with Haze-Line atmospheric light estimating [1], the results provide a surprisingly well dehazing results with rich hue information and clear details beyond other methods. Therefore, in the following testing, our iterative dehazing method will adopt the Haze-Line for the atmospheric light estimating.

More details of the atmospheric light estimating using haze-line algorithm can be referred from [1] and [9].

### 1.3. Atmospheric light estimating methods

As demonstrated in Table 1.

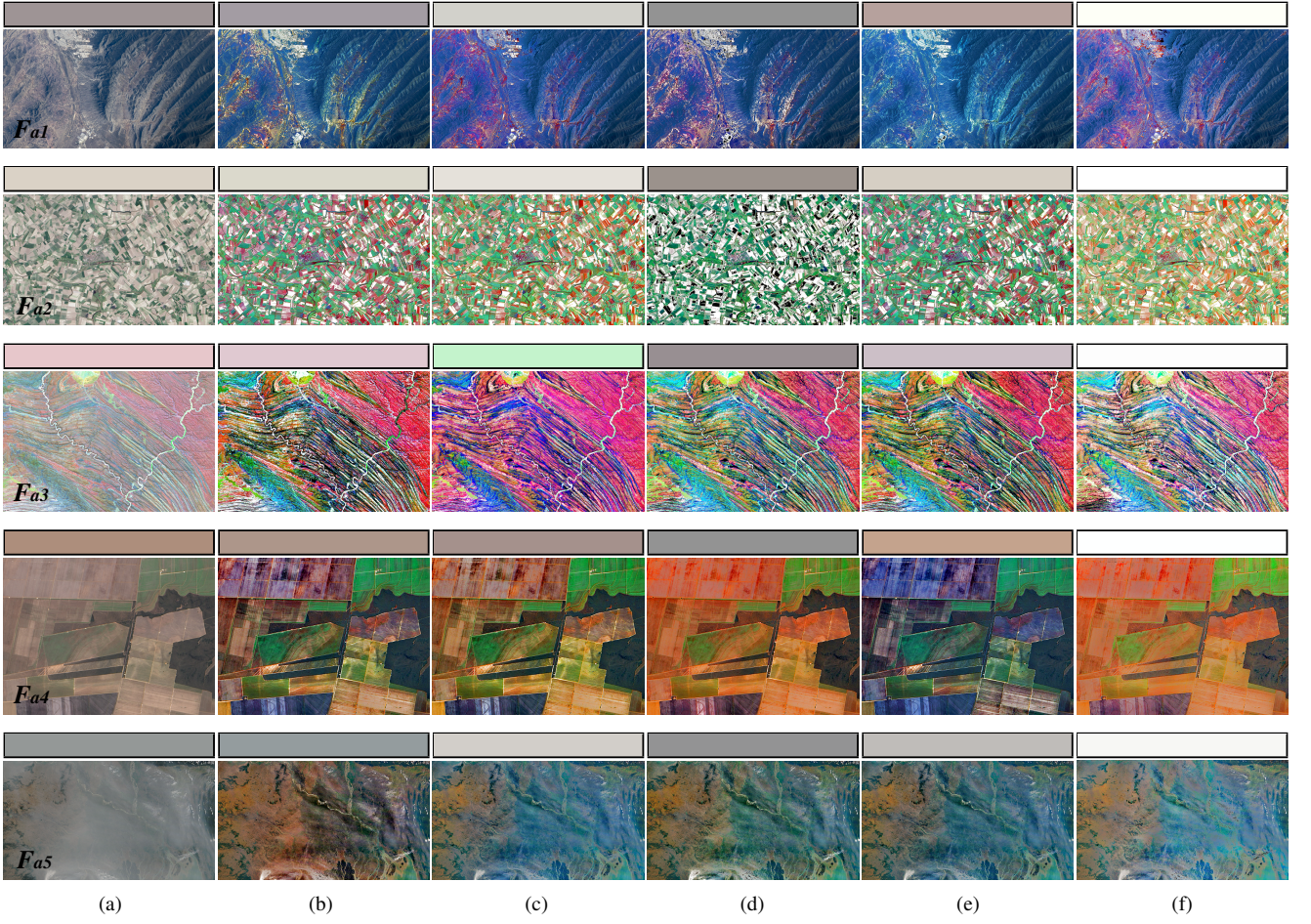


Figure 1: Evaluating the accuracy of the estimated atmospheric light on remote sensing images. (a): the hazy images. (b)-(f): the results of our iterative dehazing method, yet with different atmospheric light estimating methods proposed by Haze-Line [1], DCP [2], Color-Line [3][4], Blind [5] and DHNet [6], respectively. The color blocks on the hazy images are their manually extracted ground-truth atmospheric light. The color blocks on dehazed images are their estimated atmospheric light.

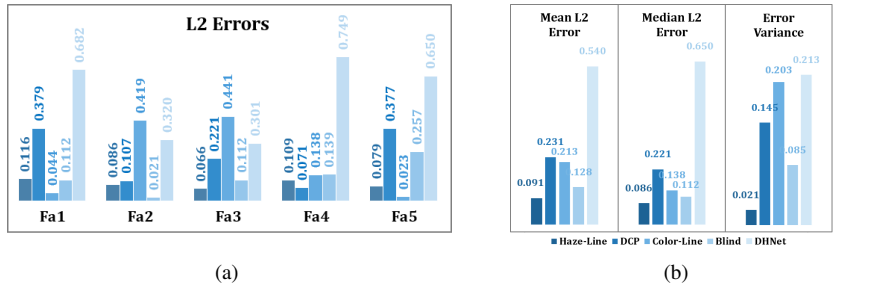


Figure 2: Evaluating the accuracy of the estimated atmospheric light on remote sensing image. (a): the  $L_2$  error for each results in Fig.1. (b): the mean  $L_2$ , median  $L_2$  and error variance results.

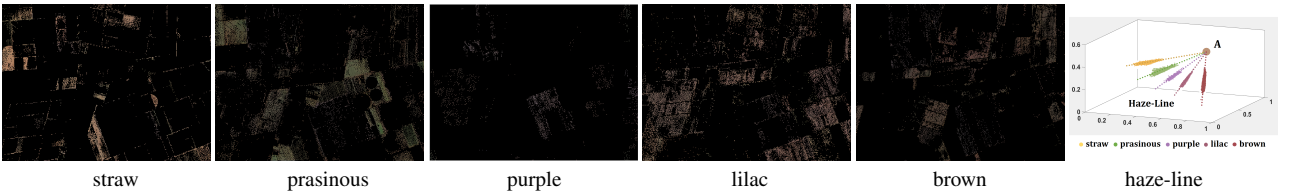


Figure 3: Five examples of haze-line. The five colors are: straw, prasinous, purple, lilac and brown, respectively. Note that the pixels are non-local and are spread all over the image plane. For clarity of display, the number of samples in haze-line figure is smaller than the actual number we use, and the angle of the five haze-lines is regulated a little.

Table 1: Comparisons of state-of-the-art dehazing methods

Methods	Method description	Complexity	Accuracy
DCP: He et al. (2009) [2]	In [2], the top 0.1% brightest pixels in the dark channel are picked up at first; then, among these pixels, the pixels with the highest intensity in the given image $\mathbf{I}$ can represent the global atmospheric light $A$ . That is, the most haze-opaque pixel was used to estimate the $A$ . However, this method is not suitable for RSI dehazing, as what aforementioned in subsection ??.	✓	✗
Color-Line: Sulami et al. (2014) [3]	separately estimate the atmospheric light magnitude and direction. The direction is estimated by looking for small patches with a constant transmission and surface albedo. Each pair of such patches provide a candidate atmospheric light direction as the intersection of two planes in RGB space. The atmospheric light magnitude is recovered by minimizing the dependence between the pixels brightness and transmission. Fattal [4] uses this atmospheric light estimation [3] for single image dehazing.	✗	✓
Blind: Bahat and Irani (2016) [5]	use internal patch recurrence prior to detect differences between such co-occurring patches and calculate the atmospheric light. The patch recurrence property is an observation that small image patches tend to repeat inside a single natural image, both within the same scale and across different scales. This property is diminished when imaging in a scattering media, since recurring patches at different distances undergo different amounts of haze and have different appearances.	✗	✓
DHNet: Cai et al. (2016) [6]	Unlike previous methods, which first estimate the global atmospheric light and use it to estimate the transmission for each pixel, the scheme suggested in [6] first estimates the transmission by DehazeNet, a convolutional neural network, and then the atmospheric light is selected as the brightest pixel whose transmission value is smaller than 0.1. Since the datasets in this method are indoor images and known depth maps, the parameters trained by these datasets are not valid for remote sensing dehazing.	✓	✗
Haze-Line: Berman et al. (2017) [1][9]	Berman et al. [1] present a fast and efficient method for estimating a global atmospheric light value in hazy images. This method is based on the haze-line prior [9] that has recently been introduced. That prior claims that pixels' intensities of objects with similar colors form lines in RGB space under haze. These lines intersect at the atmospheric light color and we take advantage of this observation to find their point of intersection.	✓	✓

## 2. APPENDIX-B: Proof on the Convergence

The iterative framework for effective transmission map refining is proposed as

$$\begin{aligned} t_c^{i+1}(\mathbf{x}) &= D_s^i(\mathbf{x}) \cdot t_{pi}(\mathbf{x}) + (1 - D_s^i(\mathbf{x})) \cdot t_c^i(\mathbf{x}) \\ &= t_c^i(\mathbf{x}) - D_s^i(\mathbf{x}) \cdot D_t^i(\mathbf{x}), \quad i = 0, 1, 2, \dots, \end{aligned} \quad (1)$$

where  $D_s^i = \mathcal{L}(D_s^i) = \mathcal{L}(t_c^i - t_{pi})$ ;  $i$  is the iteration index.  $i = 0$  indicates the initialization stage, and  $t_c^0$  is  $t_{pa}$ .

For simplicity, we omit the expression of  $\mathbf{x}$ , i.e. let  $t_c^i(\mathbf{x}) = t_c^i$ ,  $D_t^i(\mathbf{x}) = t_c^i - t_{pi} = D^i$ ,  $D_s^i(\mathbf{x}) = \mathcal{L}[t_c^i - t_{pi}] = D_s^i$ .

Firstly, we proof  $t_c^i \geq t_{pi}$  for each  $i$ .

*Proof.*

1°: Since

$$\begin{aligned} t_{pa} &= 1 - \min_{\Omega} \left[ \min_{c \in \{r,g,b\}} [I_{\Omega}^c / A^c] \right], \\ t_{pi} &= 1 - \min_{c \in \{r,g,b\}} [I^c / A^c], \end{aligned} \quad (2)$$

therefore, we have  $t_{pa} \geq t_{pi}$ . Then  $0 \leq D_s^1 = \mathcal{L}[t_{pa} - t_{pi}] \leq 1$ .

2°: Assume  $t_c^{k-1} \geq t_{pi}$  and  $0 \leq D_s^{k-1} = \mathcal{L}[t_c^{k-1} - t_{pi}] \leq 1$ . According the iterative model of (1), we have:

$$\begin{aligned} t_c^k &= D_s^{k-1} \cdot t_{pi} + (1 - D_s^{k-1}) \cdot t_c^{k-1} = t_c^{k-1} - (t_c^{k-1} - t_{pi}) \cdot D_s^{k-1} \Rightarrow \\ t_c^k - t_{pi} &= t_c^{k-1} - t_{pi} - (t_c^{k-1} - t_{pi}) \cdot D_s^{k-1} \geq 0 \Rightarrow t_c^k \geq t_{pi}. \end{aligned} \quad (3)$$

3°: Let  $k = i$  in (3), we can proof that  $t_c^i \geq t_{pi}$ .  $\square$

Then, we proof that the iterative model of (1) is convergent.

*Proof.*

Calculating the  $t_i$  for each iterations:

$$\begin{aligned} t_c^i &= t_c^i; \\ t_c^{i+1} &= D_s^i \cdot t_{pi} + (1 - D_s^i) \cdot t_c^i = t_c^i - (t_c^i - t_{pi}) \cdot D_s^i; \end{aligned} \quad (4)$$

Calculating the first derivative  $\Delta_i^1$  between each iterations:

$$\Delta_i^1 = t_c^{i+1} - t_c^i = -(t_c^i - t_{pi}) \cdot D_s^i \leq 0; \quad (5)$$

That is, the iteration is a monotone decreasing function. Since  $t_c^i \geq t_{pi}$ , therefore,  $t_c^i$  must gradually approach a point, assumed as  $t_c^{\zeta}$ , and  $t_c^{\zeta} \in [t_{pi}, t_c^{\infty}]$ . As the  $t_c^i \rightarrow t_c^{\zeta}$ , the first derivative must  $\rightarrow 0$ , that is

$$-(t_c^i - t_{pi}) \cdot D_s^i \rightarrow 0, \quad \text{when } i \rightarrow \infty. \quad (6)$$

Since  $D_s^i \geq 0$ , we have

1°: when  $D_s^i > 0$ ,

$$-(t_c^i - t_{pi}) \rightarrow 0 \Rightarrow t_c^i \rightarrow t_{pi}, \quad \text{when } i \rightarrow \infty. \quad (7)$$

2°: when  $D_s^i = 0$ , we have

$$\mathcal{L}[t_c^i - t_{pi}] = 0 \Rightarrow \text{Sig}[\text{Gau}[t_c^i - t_{pi}]] = 0. \quad (8)$$

According the feature of Sigmoid function and Gaussian filtering,  $\text{Sig}[\text{Gau}[t_c^i - t_{pi}]] = 0$ , only when  $t_c^i - t_{pi} = 0$ .

To sum up 1° and 2°, we proof that  $t_c^i \rightarrow t_{pi}$ , when  $i \rightarrow \infty$ .  $\square$

From now on, we proof that the iterative model of (1) is convergent, and with the iteration increasing,  $t_c^{\infty} \rightarrow t_{pi}$ .

## References

- [1] D. Berman, T. Treibitz, S. Avidan, Air-light estimation using haze-lines, in: Computational Photography (ICCP), 2017 IEEE International Conference on, IEEE, 2017, pp. 1–9.
- [2] K. He, J. Sun, X. Tang, Single image haze removal using dark channel prior, IEEE Transactions on Pattern Analysis & Machine Intelligence 33 (12) (2011) 2341.
- [3] M. Sulami, I. Glatzer, R. Fattal, M. Werman, Automatic recovery of the atmospheric light in hazy images, in: Computational Photography (ICCP), 2014 IEEE International Conference on, IEEE, 2014, pp. 1–11.
- [4] R. Fattal, Dehazing using color-lines, ACM Transactions on Graphics 34 (1) (2014) 1–14.
- [5] Y. Bahat, M. Irani, Blind dehazing using internal patch recurrence, in: Computational Photography (ICCP), 2016 IEEE International Conference on, IEEE, 2016, pp. 1–9.
- [6] B. Cai, X. Xu, K. Jia, C. Qing, D. Tao, Dehazenet: An end-to-end system for single image haze removal, IEEE Transactions on Image Processing 25 (11) (2016) 5187–5198.
- [7] R. T. Tan, Visibility in bad weather from a single image, in: Computer Vision and Pattern Recognition, 2008. CVPR 2008. IEEE Conference on, 2008, pp. 1–8.

- [8] R. Fattal, Single image dehazing, *Acm Transactions on Graphics* 27 (3) (2008) 1–9.
- [9] D. Berman, T. Treibitz, S. Avidan, Non-local image dehazing, in: *IEEE Conference on Computer Vision and Pattern Recognition*, 2016, pp. 1674–1682.